

# The influence of fire and permafrost on sub-arctic stream chemistry during storms

K. C. Petrone,<sup>1\*</sup> L. D. Hinzman,<sup>1</sup> H. Shibata,<sup>2</sup> J. B. Jones<sup>3</sup> and R. D. Boone<sup>3</sup>

<sup>1</sup> Water and Environmental Research Center, University of Alaska Fairbanks, Fairbanks, AK, USA

<sup>2</sup> Northern Forestry and Development Office, Field Science Center for Northern Biosphere, Hokkaido University, 250 Tokuda, Nayoro 096-0071, Japan

<sup>3</sup> Institute of Arctic Biology, University of Alaska Fairbanks, Fairbanks, AK, USA

## Abstract:

Permafrost and fire are important regulators of hydrochemistry and landscape structure in the discontinuous permafrost region of interior Alaska. We examined the influence of permafrost and a prescribed burn on concentrations of dissolved organic carbon (DOC), dissolved organic nitrogen (DON) and other solutes ( $\text{NO}_3^-$ ,  $\text{Ca}^{2+}$ ,  $\text{K}^+$ ,  $\text{Mg}^{2+}$ ,  $\text{Na}^+$ ) in streams of an experimentally burned watershed and two reference watersheds with varying extents of permafrost in the Caribou–Poker Creeks Research Watershed in interior Alaska. The low-permafrost watershed has limited permafrost (3%), the high-permafrost watershed has extensive permafrost (53%), and the burn watershed has intermediate permafrost coverage (18%). A three end-member mixing model revealed fundamental hydrologic and chemical differences between watersheds due to the presence of permafrost. Stormflow in the low-permafrost watershed was dominated by precipitation and overland flow, whereas the high-permafrost watershed was dominated by flow through the active layer. In all watersheds, organic and groundwater flow paths controlled stream chemistry: DOC and DON increased with discharge (organic source) and base cations and  $\text{SO}_4^{2-}$  (from weathering processes) decreased. Thawing of the active layer increased soil water storage in the high-permafrost watershed from July to September, and attenuated the hydrologic response and solute flux to the stream. The FROSTFIRE prescribed burn, initiated on 8 July 1999, elevated nitrate concentrations for a short period after the first post-fire storm on 25 July, but there was no increase after a second storm in September. During the July storm, nitrate export lagged behind the storm discharge peak, indicating a flushing of soluble nitrate that likely originated from burned soils. Copyright © 2006 John Wiley & Sons, Ltd.

KEY WORDS active layer; boreal forest; DOC; DON; fire; groundwater; mixing model; hysteresis; nitrate; permafrost; stream; watershed

Received 16 November 2004; Accepted 19 October 2005

## INTRODUCTION

In the discontinuous permafrost region of interior Alaska, hydrochemical processes are controlled by the distribution of permafrost. Permafrost limits hydrologic flow on north-facing slopes and in low-lying valley bottoms to the organic-rich active layer, whereas on south-facing slopes the water can infiltrate into deeper groundwater flow paths (Woo, 1986). Consequently, streams in watersheds dominated by permafrost tend to have higher dissolved organic carbon (DOC) and dissolved organic nitrogen (DON), but lower dissolved mineral concentrations than watersheds that are mostly permafrost free (Ray, 1988; MacLean *et al.*, 1999). The depth of the active layer, that portion of soil above permafrost that freezes and thaws annually, increases throughout the summer, further complicating stream chemistry patterns. Water movement and storage, as well as root and heterotrophic respiration, occur almost exclusively in this seasonally thawed layer. Because of greater water storage capacity,

an increase in active layer thickness attenuates the hydrologic response of streams to precipitation inputs (McNamara *et al.*, 1997). Changes in the depth to permafrost, therefore, affect both hydrologic and biotic processes.

Variation in stream chemistry is most pronounced during storms. Precipitation infiltrates into soils, or moves directly to the stream channel over saturated soils in the riparian zone. Consequently, source areas may differ depending on the mechanism that generates flow (Eshleman *et al.*, 1993). Water that composes the hydrograph peak may be ‘old’ water that has been displaced by precipitation or ‘new’ water from a more direct flow path to the stream (Sklash and Farvolden, 1979). In some watersheds, it is necessary to separate flow into three components if a substantial ‘surface storage’ is present, creating a perched water table (Mulholland *et al.*, 1993). In the discontinuous permafrost region, a three-component model may be appropriate, since sub-permafrost groundwater, supra-permafrost soil water, and direct precipitation generate streamflow (Woo, 1986). Regardless of source, storm water differs from baseflow because it takes a different path through watersheds and to the stream. Chemical constituents, such as DOC, may increase in streams due to the mobilization of compounds in soils that become saturated. Other elements may decline during

\* Correspondence to: K. C. Petrone, Ensis, Commonwealth and Scientific Research Organisation (CSIRO), Wembley, Western Australia, Australia. E-mail: kevin.petrone@csiro.au

storms due to the dilution of baseflow chemistry. Nutrients that are biologically reactive may show more complex patterns, depending on the season and the activity of plants and microbes.

Climate models predict an increase in fire severity and frequency in boreal forests (Flannigan and Van Wagner, 1991). The current extent of permafrost coverage is susceptible to wildfire disturbance because fire removes the insulating organic layer from the forest floor, thereby accelerating heat flux to soils, and increasing the active layer depth (Burn, 1998). Thawing of ice-rich soils can lead to ground slumping (thermokarst) and forest deterioration (Osterkamp and Romanovsky, 1999). Wildfire disturbance has been shown to increase water runoff (Wright, 1976; Schindler *et al.*, 1980; Bayley and Schindler, 1991), sediment losses (Beaty, 1994), and concentrations of major ions and DOC (Bayley and Schindler, 1991; Bayley *et al.*, 1992; Chorover *et al.*, 1994; Williams and Melack, 1997; Williams *et al.*, 1997). However, owing to variations in burn severity, soil fertility, and the spatial extent of burn areas, effects on stream chemistry and hydrology can be limited or undetectable (Richter *et al.*, 1982). Fire severity plays a particularly important role in interior Alaska. Severe fires can completely burn through the insulating moss layer, causing permafrost to thaw, resulting in improved drainage to the mineral soil below (Hinzman *et al.*, 2003). However, less severe fires may only burn the surface layer, leaving the underlying organic layer intact. Where burning occurs, organic plant biomass is converted into inorganic forms as an ash on the forest floor and exposes organic soils to erosion.

In this study, we examined the role of permafrost and fire on short-term watershed solute fluxes. This research was conducted at the Caribou–Poker Creeks Research Watershed (CPCRW) in interior Alaska as part of a multidisciplinary fire disturbance project called FROSTFIRE (Hinzman *et al.*, 2003). We monitored stream chemistry in an experimentally burned watershed with moderate permafrost coverage and two reference watersheds with low and high permafrost coverage during the summer of 1999 before and after the fire. Our objectives were to determine the influence of permafrost on (i) the composition of storm water to the hydrograph and (ii) the contributing area for streamflow. Lastly, the understanding gained from these objectives will be used to elucidate the immediate effect of fire on stream chemistry. We hypothesized that, in the watershed with greater permafrost coverage, the total amount of storm (precipitation and organic soil) water to streamflow would increase due to a greater contribution from organic soil flow pathways. By examining three watersheds with differing amounts of permafrost, we attempt to determine the mechanisms that generate streamflow and chemistry.

#### STUDY SITE

The CPCRW, part of the Bonanza Creek LTER, is located 50 km northeast of Fairbanks, Alaska, and covers 10

620 ha. The climate is continental, with low winter temperatures, high summer temperatures, and an annual mean temperature of  $-2.5^{\circ}\text{C}$ . The average annual precipitation for the region ranges from 285 mm for Fairbanks to near 500 mm in upper elevations of CPCRW. Roughly half of the precipitation falls as snow. Snowmelt typically starts in late April and lasts for 3 to 5 weeks. During the snow-free period, May and June have the lowest precipitation and July through to September have greater rainfall.

The CPCRW boundary includes several sub-basins that differ in permafrost coverage due to aspect (Figure 1). Low sun angles throughout the year result in less energy reaching slopes with northern aspects than slopes with southern aspects. Vegetation is closely related to soil type and permafrost distribution. North-facing slopes are dominated by a black spruce (*Picea mariana*) and feather moss (*Pleurozium schreberi*) community, whereas south slopes are deciduous with a mixture of quaking aspen (*Populus tremuloides*) and paper birch (*Betula papyrifera*). Permafrost is also found in riparian zone or valley bottom sites adjacent to the stream due to persistent temperature inversions throughout the winter and poorly drained soils in this zone (Yoshikawa *et al.*, 2002). Maximum depth of thaw on permafrost hillslopes can reach  $>1$  m, whereas poorly drained sites thaw to only 0.5 m in September prior to refreezing. Bedrock is unconsolidated Birch Creek schist with surface soils composed of Fairbanks silt loam that have developed in fine loess transported from the Alaska Range.

Three watersheds were examined in this study. The burn watershed has a moderate amount of permafrost (18.8%) and a watershed area of 1040 ha. The two reference watersheds had high (53.2%) and low permafrost (3.5%) and areas of 520 ha and 570 ha respectively (Rieger *et al.*, 1972). A prescribed burn was conducted on 8–15 July 1999 by the Bureau of Land Management and the Alaska Fire Service that moderately to severely burned approximately 28% (320 ha) of the burn watershed (Hinzman *et al.*, 2003). The burn area was limited primarily to the north-facing, black-spruce-covered slope of the watershed. However, a smaller southeast-facing

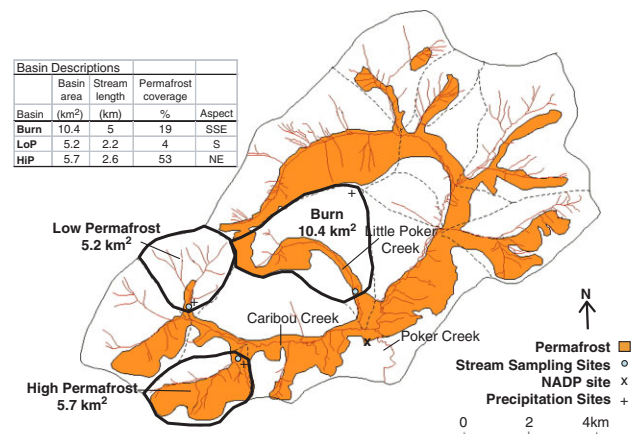


Figure 1. Permafrost and site descriptions at the CPCRW, including the burn, low-permafrost (LoP) and high-permafrost (HiP) watersheds (Haugen *et al.*, 1982)

section was hand ignited by fire crews within 2 days of the initial burn. Despite a large burn area, much of the riparian zone with saturated soils was unburned.

## METHODS

Stream discharge was measured continuously from late April through to September 1999 in all three streams and periodically throughout the winter when the streambed was ice free. Stream stage was recorded every hour with a 5 psi pressure transducer and a Campbell datalogger (CR10X). The pressure transducer was removed during the fire, reinstalled after the fire, and subsequently recorded every 0.5 h. Periodic discharge measurements were estimated with a Marsh–McBirney electromagnetic current meter to calculate a rating curve and convert stage height to discharge. Precipitation for the July storm was calculated from tipping buckets in the low-permafrost and high-permafrost watersheds. Precipitation in the burn watershed in July and all watersheds in September was calculated from a remote automated weather station (RAWS; <http://fire.ak.blm.gov/>) maintained by the Bureau of Land Management, located at Caribou Peak on the boundary of the burn watershed.

Stream water for chemical analyses was collected with an ISCO autosampler every 4 h in the high-permafrost and low-permafrost watersheds, and every 2 h in the burn watershed during storms. Samples remained in autosamplers for up to 4 days between collections. We found that certain chemistry, such as pH and  $\text{NH}_4^+$ , did change during this storage period, but we did not use these stored samples for storm chemistry. Otherwise, we found no significant difference between those samples collected by the autosampler and stored for the 4-day period and those samples that were collected manually at the same time and frozen or refrigerated before analysis. Samples were transferred to pre-rinsed 125 ml HDPE bottles in the field and filtered within 12 h using glass-fibre filters (Gelman AE, 0.45  $\mu\text{m}$  nominal pore size). Samples were refrigerated until analysis (<48 h) or frozen for subsequent analyses. Electrical conductivity was measured in the laboratory using a hand-held Denver Instruments AP-50 meter. An Alpkem autoanalyser was used to measure  $\text{NH}_4^+$  by the phenol–hypochlorite method (Solorzano, 1969), soluble reactive phosphorus (SRP) by the molybdate–antimony method (Murphy and Riley, 1962), and  $\text{NO}_3^-$  by cadmium reduction (Wood *et al.*, 1967). DOC was measured as non-purgeable organic carbon on a Shimadzu TOC 5000. Base cations and anions ( $\text{Ca}^{2+}$ ,  $\text{K}^+$ ,  $\text{Mg}^{2+}$ ,  $\text{Na}^+$ , and  $\text{SO}_4^{2-}$ ) were analysed using inductively coupled plasma optical emission spectrometry (Jarrel Ash Inc., IRIS) at the North Research Station of Hokkaido University Forests (NR-HUF), Japan.

We determined water sources during storms using an end-member mixing analysis (EMMA) that separates flow into source components using a mass balance of water and hydrochemical tracers (Hooper and Shoemaker, 1986). Hydrologic studies commonly separate

flow of storm discharge peaks into ‘new’ (i.e. precipitation) and ‘old’ (i.e. groundwater) water components using a two end-member approach. An important assumption of two end-member separation is that surface soil water components have little storage (Sklash *et al.*, 1976). Because permafrost creates ‘surface storage’ as a perched water table in the dominant organic soil flow path, we used a three-component separation model (DeWalle *et al.*, 1988). DOC and calcium were used as tracers because they showed the largest separation among model components; DOC is high in organic surface soils but low in groundwater, mineral soil, and precipitation, whereas calcium shows the opposite pattern due to weathering in mineral soil and bedrock. In this study, we separated flow into three components: (1) precipitation, (2) organic soil, and (3) groundwater:

$$f_{\text{gw}} + f_{\text{org}} + f_{\text{precip}} = 1 \quad (1)$$

$$[\text{Ca}]_{\text{gw}}f_{\text{gw}} + [\text{Ca}]_{\text{org}}f_{\text{org}} + [\text{Ca}]_{\text{precip}}f_{\text{precip}} = [\text{Ca}]_{\text{stream}} \quad (2)$$

$$\text{DOC}_{\text{gw}}f_{\text{gw}} + \text{DOC}_{\text{org}}f_{\text{org}} + \text{DOC}_{\text{precip}}f_{\text{precip}} = [\text{DOC}]_{\text{stream}} \quad (3)$$

where [Ca] and [DOC] are end-member concentrations,  $f$  is the fraction of each component contributing to streamwater, and the subscripts precip, org, gw, and stream represent precipitation, organic soil, groundwater, and streamwater respectively. The above equations were solved for each time we collected stream chemistry during a storm, and periods between samples were linearly interpolated. The total storm contribution for any given component equals the sum over the stormflow period.

The  $\text{Ca}^{2+}$  concentration in wet deposition from the on-site National Atmospheric Deposition Site (site AK01; <http://nadp.sws.uiuc.edu/>) was used for the precipitation signature during both storms. We used the weekly averages (20–27 July 1999 and 31 August–9 September) as signatures for each storm. DOC concentrations in precipitation were assumed to be equal to zero.  $\text{Ca}^{2+}$  and DOC concentrations in soils were determined by lysimeters installed in the burn watershed. Zero-tension (three burn and three control,  $n = 6$ ) and suction lysimeters (20 burn and 20 control,  $n = 40$ ) were installed in 1998 along transects extending from the toe slope to the riparian zone in spruce stands in the burn watershed prior to the fire event. Hardwood (aspens and birch) stands on the south side of the stream yielded little water in lysimeters and are likely a small component of organic soil flow during the summer period. Zero-tension lysimeters were installed in the Oa horizon, which consisted of a thick layer (>10 cm) of decomposed moss and plant litter. Tension lysimeters made of porous ceramic cups (Soil Moisture Inc. and Prenart Inc.) were installed at the interface between the organic and mineral horizons (between 20 and 30 cm depth). We were unable to measure the immediate effect of the fire in the tension lysimeters because they were

frozen in the ground and could not be removed prior to the fire. Consequently, the lysimeters were destroyed during the burn. Those lysimeters that were unburned were sampled after the fire in 1999. Final end-member signatures were obtained by taking an average of all lysimeters from 1998 and the unburned lysimeters during 1999. There was no significant difference between years. We did not collect soil water samples in the low- and high-permafrost watersheds, but mean concentrations of  $\text{Ca}^{2+}$  and DOC in spruce stands from MacLean *et al.* (1999) in these watersheds were not significantly different from  $\text{Ca}^{2+}$  and DOC in the burn watershed. The same groundwater signature was used for all three watersheds by obtaining an average concentration for DOC and  $\text{Ca}^{2+}$  from seeps, wells and pingo springs from the CPRW ( $n = 13$ ; White *et al.*, 2002). These average concentrations represent an estimate of the regional groundwater signature at CPRW.

A sensitivity analysis was performed on EMMA by incorporating sample variability and analytical error in end-member signature estimates. We calculated the standard error of the organic and groundwater end-member concentrations and ran the model using plus and minus the standard error of the mean. Since only one sample was available for the precipitation signature for each storm, we used the analytical error of replicate samples (Gordon, 1999). We ran the model by varying end-members individually using the high and low range of the end-member signatures. These model outputs were compared with the original model run using the mean end-member signature.

Linear regressions were performed on chemical concentrations versus discharge for the July and September storms. Normal probability plots of residuals from regressions were used to test the assumptions of normality. In all cases, stream data conformed to residual normality tests, except for nitrate and sulphate in the burn watershed in July (StatSoft, 2000). Transformations did not significantly improve the distribution of nitrate and sulphate regressions, so we report raw data for all regressions. Regressions were compared between July and September storms using a *t*-test on regression slopes (Sokal and Rohlf, 1994). Contributing areas were calculated by separating the hydrograph into the groundwater, organic, and precipitation flow components, and dividing the precipitation discharge by the total precipitation for the storm event (Table II; Eshleman *et al.*, 1993). Since the precipitation component of flow has little interaction with subsurface soils, saturation overland flow likely generates this discharge during the storm event, as outlined by Eshleman *et al.* (1993).

## RESULTS

Total precipitation amounts were comparable for the July and September storms (22.6 mm and 22.9 mm respectively), but maximum precipitation intensity was lower during the July storm ( $11.4 \text{ mm h}^{-1}$ ) compared

to the September storm ( $22.4 \text{ mm h}^{-1}$ ). As a result, storm discharge peaks in the burn and low-permafrost watersheds were lower in July. In contrast, the high-permafrost watershed showed the greatest discharge peak in July and declined to less than half of this amount in September (Figure 2). Peak flows for the July storm in high permafrost ( $129 \text{ l s}^{-1}$ ) and the burn watershed ( $107 \text{ l s}^{-1}$ ) were four- to five-fold greater than the low-permafrost basin discharge ( $26 \text{ l s}^{-1}$ ). In September, peak flow remained high in the burn watershed ( $150 \text{ l s}^{-1}$ ) and low in the low-permafrost watershed ( $43 \text{ l s}^{-1}$ ), whereas the high permafrost watershed peak discharge was much lower than July ( $55 \text{ l s}^{-1}$ ). The time to peak from precipitation to the storm discharge maximum was shorter overall in September except for the high permafrost watershed, which took several hours longer to peak than the other watersheds. In July, the burn and high-permafrost watersheds peaked similarly, whereas the low-permafrost peak was earlier (Figure 2).

Baseflow chemistry prior to the prescribed burn was consistent for each watershed and reflects the stream-specific contribution of groundwater versus soil flow paths. The DOC concentration was highest in the high-permafrost watershed ( $1341 \mu\text{M}$ ), intermediate in the

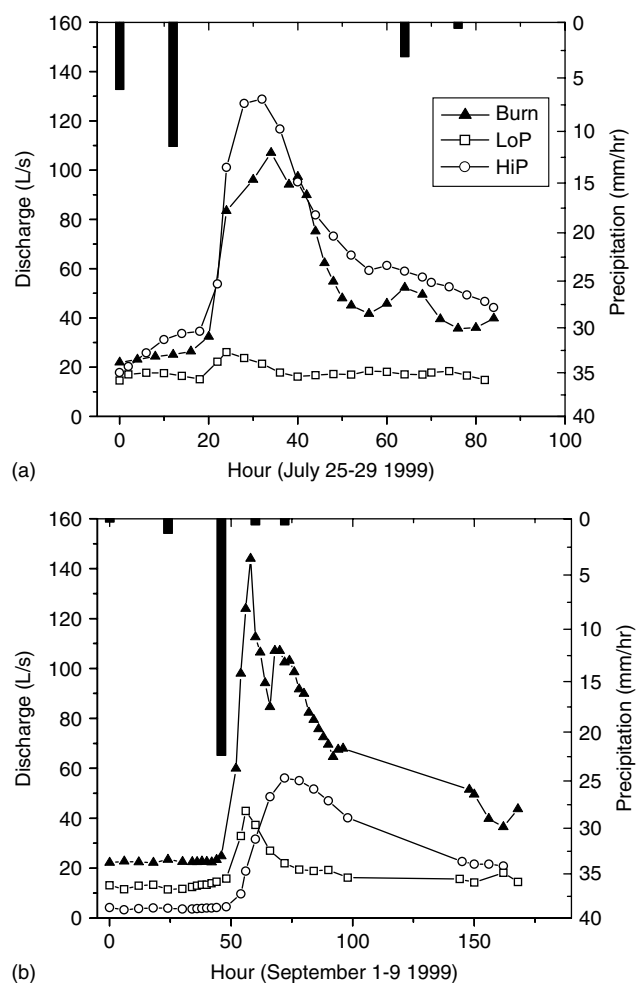


Figure 2. Precipitation and discharge for the burn (closed triangles), low-permafrost (LoP: open squares), and high-permafrost (HiP: open circles) watersheds for the (a) July and (b) September storms

Table I. Pre-fire chemistry of surface stream water in the burn, low-permafrost (LoP), and high-permafrost (HiP) watersheds during baseflow conditions, June 1999

	Burn		LoP		HiP	
	Mean	SE	Mean	SE	Mean	SE
Conductivity ( $\mu\text{S cm}^{-1}$ )	101	0.4	68	0.1	50	0.8
Nitrate ( $\mu\text{M}$ )	45.4	0.3	40.6	0.1	21.8	0.1
Ammonium ( $\mu\text{M}$ )	1.1	0.2	1.3	0.3	0.9	0.2
Phosphate ( $\mu\text{M}$ )	0.5	0.0	0.4	0.0	0.3	0.0
DOC ( $\mu\text{M}$ )	357	8.1	594	11.1	1341	10.6
DON ( $\mu\text{M}$ )	53.1	2.0	41.2	1.3	50.4	0.4
DOC/DON	6.7	—	14.4	—	26.6	—
DON/DIN	1.2	—	1.0	—	2.3	—

low-permafrost watershed (594  $\mu\text{M}$ ), and lowest in the burn watershed (357  $\mu\text{M}$ ; Table I). Conversely, electrical conductivity, a measure of total dissolved solutes, was highest in the burn watershed (101  $\mu\text{S}$ ), intermediate in the low-permafrost watershed (68  $\mu\text{S}$ ), and lowest in the high-permafrost watershed (50  $\mu\text{S}$ ). Ammonium (near 1  $\mu\text{M}$  for all streams) and SRP ( $<1 \mu\text{M}$ ) were consistently low in all streams and were often below detection limits. Nitrate, highest in the burn watershed (45.4  $\mu\text{M}$ ), intermediate in the low-permafrost watershed (40.6  $\mu\text{M}$ ), and lowest in the high-permafrost watershed (21.8  $\mu\text{M}$ ), was 20- to 40-fold greater than ammonium and comprised nearly all of the dissolved inorganic nitrogen (DIN) output from the CPCRW watersheds. On an annual basis, nitrate concentrations were lowest for all streams during mid-May at the peak of snowmelt. This snowmelt dilution of nitrate was greatest in the high-permafrost watershed, where nitrate approached 0  $\mu\text{M}$  (Figure 3).

### Three end-member analysis

The stream concentrations for DOC and  $\text{Ca}^{2+}$  fell within the bounds of the end-members in the mixing diagram (Figure 4a and b), indicating that the stream water was indeed a mixture of flow from three components. For all streams, the concentrations of DOC and  $\text{Ca}^{2+}$  moved closer to the organic soil end-member during storms, indicating an increase in the soil component. The trajectory of the  $\text{Ca}^{2+}$  and DOC relationship was clockwise for all watersheds in July, whereas in September the trajectory was counter-clockwise (Figure 4a and b). Mixing-model calculation revealed that the high-permafrost basin received the greatest contribution from organic soils, whereas the low-permafrost basin had the smallest organic contribution during both events (Figure 5). In July, groundwater dominated the hydrograph in the burned watershed, both precipitation and groundwater dominated the low-permafrost hydrograph, and the organic soil component dominated the high-permafrost hydrograph. Groundwater continued to dominate the burn hydrograph in September, and it also composed most of the low- and high-permafrost hydrographs (Figure 5). All watersheds showed a decline in

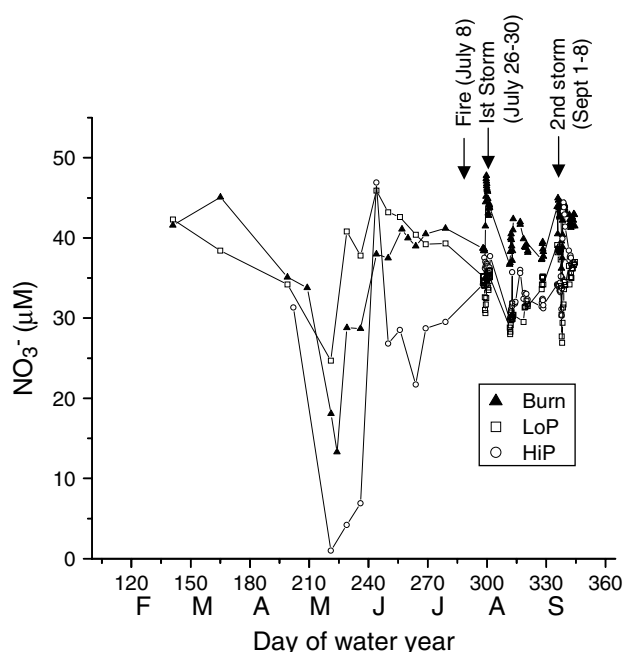


Figure 3. Annual pattern of nitrate concentration for the three watersheds: burn (closed triangles), low-permafrost (LoP: open squares) and high-permafrost (HiP: open circles) watersheds

the organic soil component with a concomitant rise in the groundwater component from July to September (Table II).

When EMMA source chemistries were changed by plus or minus a standard error, the sensitivity analysis showed a  $<10\%$  change in the relative proportions of flow components to storms. The three end-member mixing model was most sensitive to variation in the calcium concentration of groundwater: with the low range of the groundwater calcium concentration the groundwater component increased 6 to 8% with a concomitant decrease in the precipitation component (5 to 7%). The model was also sensitive to the concentration of DOC in the organic soil component. A standard error increase in the soil DOC concentration resulted in a drop in the organic soil component of 1 to 3% and an increase in precipitation flow (1–3%). All other variations in end-member concentrations tested produced little change in the model outcome ( $<1\%$ ). These potential sources of error were small compared with the differences among watersheds.

### Hydrograph separation and contributing areas

The groundwater component dominated the hydrograph in both events except for the low-permafrost and high-permafrost watersheds in July, when the precipitation and organic components were greatest (Figure 5). Compared with July, the September storm showed an increase in the groundwater component and a decrease in the organic component (Table II). Similarly, the precipitation component increased in the burn and high-permafrost watersheds, but decreased slightly in the low-permafrost watershed between July and September.

With the increased precipitation intensity in the September storm, the total storm contributing areas

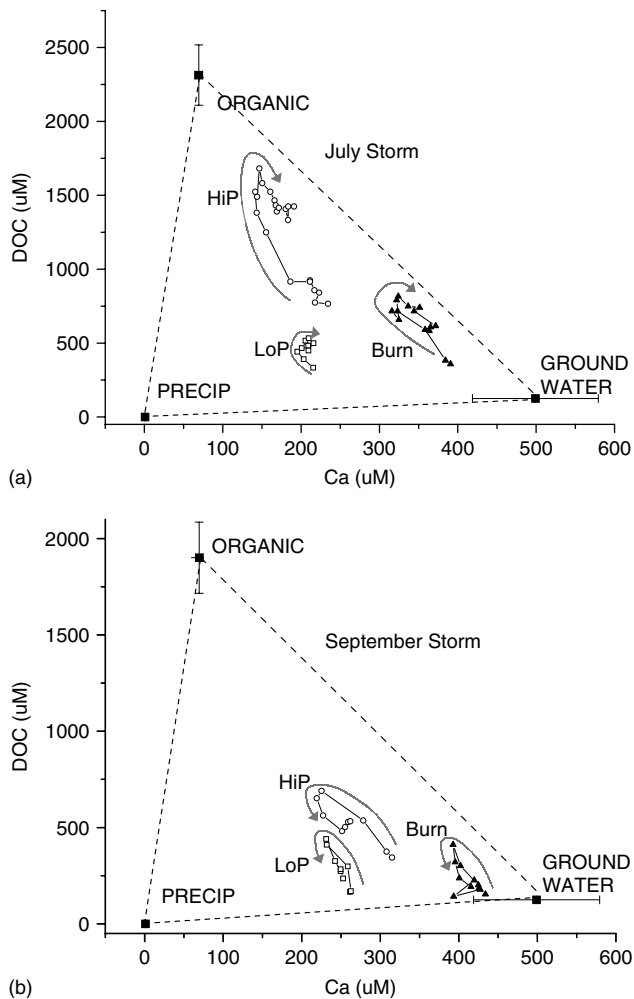


Figure 4. Mixing diagram using DOC and calcium as end-members with the burn (closed triangles), low-permafrost (LoP: open squares) and high-permafrost (HiP: open circles) stream concentrations during the (a) July and (b) September storms. The closed squares of the mixing triangle represent the end-member concentrations and error bars ( $\pm$ SE)

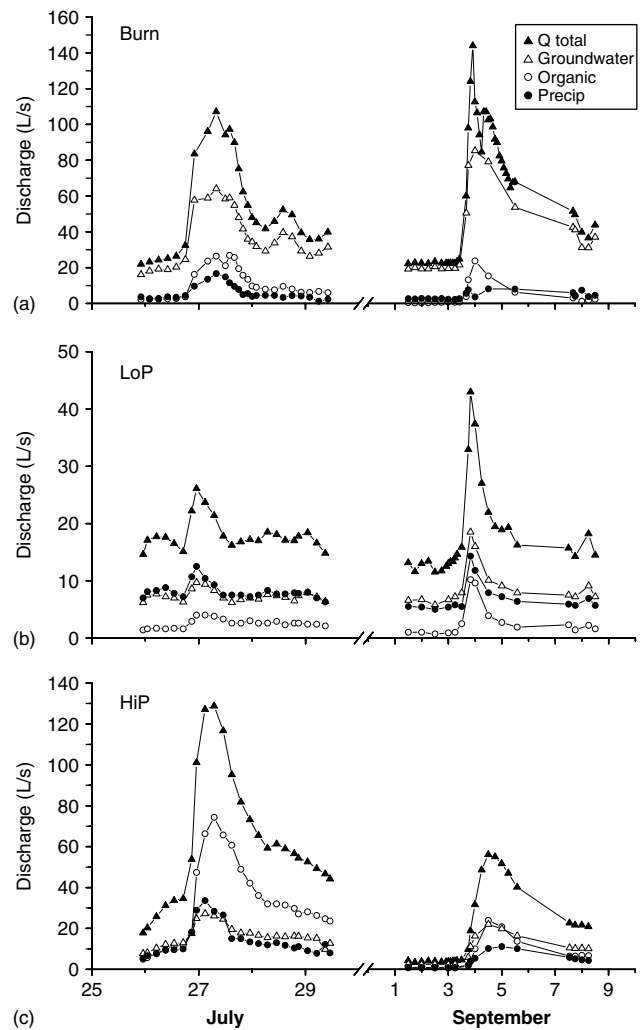


Figure 5. Contribution of the Precip (precipitation), organic, and groundwater components to the total discharge for the (a) burn, (b) low-permafrost and (c) high-permafrost basins during the July and September storm events

increased in the low-permafrost watershed (3.5 to 9.1 ha) and burned watershed (5.5 to 13.8 ha). In contrast, the high-permafrost watershed contributing area increased

only slightly from 13.6 to 14.7 ha, due to an increase in soil storage. As a percentage of the watershed area, the total storm contributing area was greatest in the

Table II. Hydrograph separation results from the three end-member mixing model for the burn, low-permafrost (LoP), and high-permafrost (HiP) watersheds for the July and September 1999 storm events<sup>a</sup>

Site	Total storm discharge (m <sup>3</sup> )	Precipitation		Discharge						TSWCA (ha)	TSWCA/Watershed area (%)
		Total (mm)	Max. (mm h <sup>-1</sup> )	Groundwater		Organic		Precipitation			
				m <sup>3</sup>	% of total	m <sup>3</sup>	% of total	m <sup>3</sup>	% of total		
<i>July</i>											
Burn	15 331	22.6	11.4	10 635	69.4	3446	22.5	1250	8.2	5.5	0.5
Low permafrost	1867	22.6	11.4	749	40.1	317	17.0	801	42.9	3.5	0.7
High permafrost	18 649	22.6	11.4	4828	25.9	10 740	57.6	3081	16.5	13.6	2.4
<i>September</i>											
Burn	28 169	22.9	22.4	22 452	79.7	2549	9.0	3168	11.2	13.8	1.3
Low permafrost	5232	22.9	22.4	2529	48.3	610	11.7	2093	40.0	9.1	1.8
High permafrost	12 808	22.9	22.4	6461	50.4	2977	23.2	3370	26.3	14.7	2.6

<sup>a</sup> Total storm water contributing area (TSWCA) = precipitation discharge/total precipitation.

high-permafrost watershed in July (14.5%) and the burn watershed (11.8%) was highest in September. The contributing area remained low in the low-permafrost watershed in both July (1.6%) and September (4.4%; Table II).

#### *Stream water chemistry and discharge relationships*

In general, the base cations, sulphate and electrical conductivity, which were most concentrated in groundwater, tended to decline during stormflows (Table III). Discharge versus concentration relationships were statistically significant in 31 of 36 of these cases. If present, hysteresis patterns were always clockwise and concentrations were lower at the end than at the beginning of the storm (e.g. Ca and K patterns in Figures 6 and 7). In contrast, DOC and DON relationships were significant positive with flow in 8 out of 12 cases for the two storms (Table III). When hysteresis patterns were present for DOC and DON, they always showed counter-clockwise patterns so that the concentration was greater at the end compared to the beginning of the storm (Figures 6 and 7). Interestingly, nitrate had both positive and negative relationships with discharge. During the July storm, nitrate was positively correlated with discharge in the burn and high permafrost basins, but negatively correlated with discharge in low permafrost (Figures 6 and 7, Table III). In the September storm, nitrate remained positive with discharge in the high-permafrost watershed and negative in the low-permafrost watershed, whereas the burn watershed changed to a negative relationship with discharge. Nitrate showed anticlockwise hysteresis loops in the burn watershed during both storms and in the high-permafrost watershed in September.

## DISCUSSION

Our results support the conceptual model hypothesized by MacLean *et al.* (1999), whereby permafrost restricts water to the active layer, reducing the modulation of DIN, DON and DOC to the stream. We expand upon this model by demonstrating that the source area for flow and the mechanism of water movement to the stream play an important role in stream chemistry during periods of high flow. Furthermore, the hydrologic and chemical responses are attenuated by an increase in active layer thickness and water storage during the summer months.

#### *Fire effects*

Numerous studies have documented elevated stream solute concentrations following fire (Bayley and Schindler, 1991; Bayley *et al.*, 1992; Chorover *et al.*, 1994; Williams and Melack, 1997; Williams *et al.*, 1997). In this study, the hysteresis pattern observed and the shift from a positive to negative nitrate versus discharge relationship suggests a possible nitrate source in the burn watershed. Compared with the reference watersheds, the burn watershed was the only stream that showed a concentration–discharge relationship with a change in

direction; the nitrate concentration–discharge relationship was positive in July but negative in September (Figures 6 and 7). The anticlockwise hysteresis of nitrate in the burn watershed in July revealed a lag response of export that may be attributed to a ‘flushing effect’ of nitrate from burned soils whereby readily soluble ions are dissolved by event water (Evans and Davies, 1998).

Nitrate dynamics in the burn watershed can be explained by the mixing model analysis and contributing area for each storm. The contributing area (5.5 ha) for the July storm likely included areas that were burned on either side of the stream. Given the large riparian saturated areas in CPCRW, a likely runoff sequence could begin with flow from the near-stream saturated soils, followed by flow from adjacent hillslope areas as soils become saturated from a perched water table in the active layer (Hooper *et al.*, 1990). Our data are consistent with such a runoff sequence: nitrate initially decreased on the rising limb of the hydrograph due to an influx of nitrate-depleted mixed precipitation and standing water from anoxic riparian soils. Subsequently, nitrate increased as runoff from the burned zones reached the stream.

#### *Permafrost and hydrology*

A comparison of the timing and magnitude of hydrographs peaks among the three watersheds suggests that permafrost plays an important role in stream water generation (Figure 2a and b). The quick and short duration response in the low-permafrost watershed likely reflects its small contributing area (5 ha in July and 12 ha in September), and confinement of flow to saturated riparian soils. Precipitation directly onto saturated areas is consistent with a rapid hydrologic response as water moved to the stream as overland saturated flow or direct channel flow (Hill, 1993). This mechanism likely generated the earlier discharge peak observed in the low-permafrost watershed compared with the burn and high-permafrost watersheds.

Temporal changes in the active layer affected discharge patterns in the high-permafrost watershed. Peak discharge in this watershed was lower in September despite greater precipitation intensity, whereas the low-permafrost and burn watersheds showed faster time to peak and higher discharge in response to this more rapid precipitation. Active layer depths increase steadily throughout the summer months, reaching a maximum in September prior to soil freeze-up (McNamara *et al.*, 1997; Hinzman *et al.*, 2006). Such a change in the active layer depth would increase soil storage and reduce the amount of water that enters the stream from precipitation because soils are slower to become saturated and generate streamflow. Since the hydraulic conductivity of thawed organic soils is high (Woo, 1986), the infiltration rate far exceeded the precipitation rate, and less runoff from permafrost-dominated hillslopes reached the stream during a late-summer storm. In contrast, the contributing areas for the low-permafrost and burn watersheds are less affected by seasonal changes in the active layer. Thawing does

Table III. Regression coefficients for stream chemical concentrations versus discharge in the burn, low-permafrost (LoP), and high-permafrost (HiP) watersheds for the July and September 1999 storm events<sup>a</sup>

Species	July						September						Event		
	Site	n	Slope	±SE	Intercept	P	n	Slope	±SE	Intercept	±SE	R <sup>2</sup>	P	t	P
NO <sub>3</sub> <sup>-</sup>	Burn	25	0.05	0.03	40.18	<0.05	40	(0.05)	0.01	45.09	0.78	0.31	<0.001	2.75	<0.01
	LoP	23	(0.42)	0.07	41.75	<0.001	25	(0.41)	0.04	42.70	0.79	0.81	<0.001	(0.10)	—
	HiP	24	0.01	0.01	35.19	<0.05	25	0.19	0.02	32.68	0.55	0.76	<0.001	(6.65)	<0.001
SO <sub>4</sub> <sup>2-</sup>	Burn	24	(0.10)	0.02	72.61	<0.001	ns	—	—	—	—	—	—	—	—
	LoP	22	(1.01)	0.18	83.12	<0.001	17	(0.46)	0.05	77.24	0.96	0.84	<0.001	(2.44)	<0.01
	HiP	23	(0.28)	0.08	60.25	<0.01	17	(0.81)	0.10	95.28	2.52	0.78	<0.001	2.94	<0.01
Conductivity (µS cm <sup>-2</sup> )	Burn	24	(0.20)	0.02	113.88	<0.001	40	(0.15)	0.01	117.84	0.39	0.95	<0.001	(1.81)	—
	LoP	23	(0.48)	0.14	87.96	<0.01	25	(0.32)	0.04	88.75	0.86	0.68	<0.001	(0.88)	—
	HiP	24	(0.24)	0.03	65.07	<0.001	25	(0.50)	0.03	88.51	0.93	0.89	<0.001	4.21	<0.001
Ca <sup>2+</sup>	Burn	25	(0.95)	0.10	417.60	<0.001	18	(0.46)	0.07	442.72	3.84	0.70	<0.001	(2.88)	<0.01
	LoP	23	(1.77)	0.56	245.85	<0.01	17	(1.00)	0.11	271.06	2.21	0.82	<0.001	(1.14)	—
	HiP	24	(0.77)	0.10	225.82	<0.001	17	(2.04)	0.21	322.39	5.08	0.85	<0.001	4.17	<0.001
Mg <sup>2+</sup>	Burn	25	(0.25)	0.03	118.78	<0.001	18	(0.12)	0.01	133.58	0.75	0.80	<0.001	(3.17)	<0.01
	LoP	23	(0.82)	0.23	122.50	<0.01	17	(0.54)	0.06	142.12	1.23	0.81	<0.001	(0.96)	—
	HiP	24	(0.17)	0.02	56.70	<0.001	17	(0.43)	0.04	80.35	0.93	0.89	<0.001	4.41	<0.001
K <sup>+</sup>	Burn	25	(0.04)	0.00	19.62	<0.001	18	ns	—	—	—	—	—	—	—
	LoP	23	(0.11)	0.03	13.31	<0.01	17	ns	—	—	—	—	—	—	—
	HiP	24	(0.03)	0.00	10.34	<0.001	17	(0.05)	0.00	10.07	0.12	0.84	<0.001	2.38	<0.05
Na <sup>+</sup>	Burn	25	(0.15)	0.02	54.49	<0.001	18	(0.09)	0.01	50.57	0.48	0.84	<0.001	(1.93)	—
	LoP	23	ns	—	—	—	17	ns	—	—	—	—	—	—	—
	HiP	24	(0.06)	0.02	38.96	<0.001	17	(0.16)	0.01	41.98	0.31	0.90	<0.001	3.08	<0.01
DON	Burn	24	0.19	0.04	46.62	<0.001	36	ns	—	—	—	—	—	—	—
	LoP	21	ns	—	—	—	15	ns	—	—	—	—	—	—	—
	HiP	23	0.14	0.03	51.08	<0.001	18	1.69	0.16	22.82	3.91	0.87	<0.001	(8.12)	<0.001
DOC	Burn	25	4.64	0.62	318.33	<0.001	40	2.42	0.09	85.06	6.66	0.95	<0.001	3.12	<0.01
	LoP	23	ns	—	—	—	18	7.58	1.29	110.29	28.08	0.65	<0.001	—	—
	HiP	24	6.09	1.41	894.17	<0.001	17	7.40	0.47	294.53	15.04	0.94	<0.001	(0.69)	—
Al <sup>3+</sup>	Burn	25	ns	—	—	—	18	ns	—	—	—	—	—	—	—
	LoP	23	ns	—	—	—	17	ns	—	—	—	—	—	—	—
	HiP	24	0.02	0.00	0.56	<0.05	17	0.01	0.00	0.70	0.04	0.51	<0.01	1.51	—
Fe	Burn	25	0.01	0.00	0.09	<0.001	11	0.00	0.00	(0.12)	0.03	0.90	<0.001	1.49	—
	LoP	23	0.02	0.00	(0.06)	<0.01	16	0.01	0.00	(0.14)	0.03	0.82	<0.001	0.48	—
	HiP	24	0.02	0.00	0.48	<0.001	17	0.02	0.00	0.03	0.02	0.94	<0.001	0.97	—

<sup>a</sup> The regression equation is  $[y] = MQ + b$ , where  $[y]$  is concentration,  $M$  is the slope and  $b$  is the intercept. SE is the standard error of the slope and intercept. Values in parentheses are negative. Concentrations are µM unless reported otherwise. A significant  $t$  statistic indicates a difference between slopes for the two storm events.

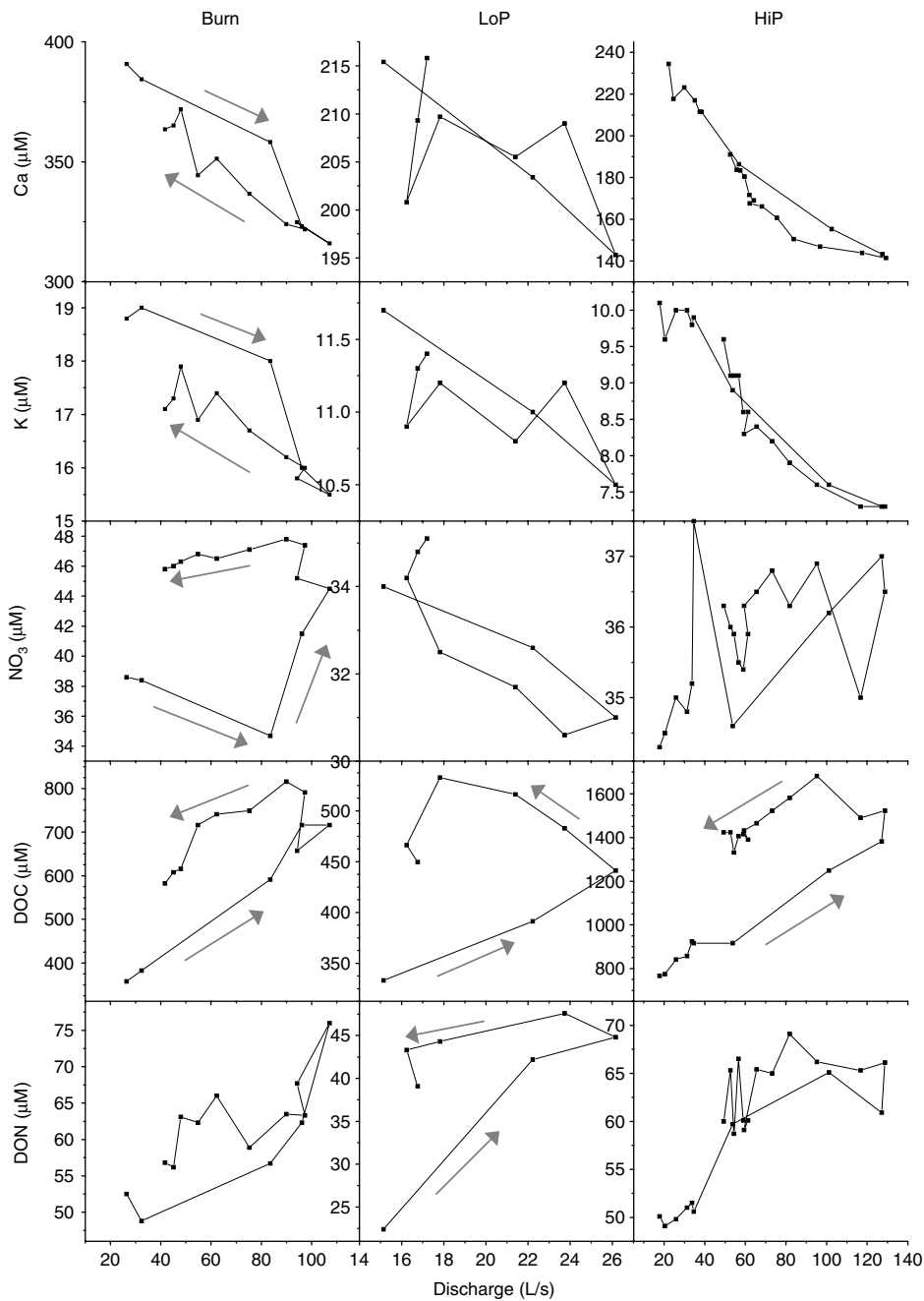


Figure 6. Concentration versus discharge plots of selected chemistry for the burn, low-permafrost (LoP) and high-permafrost (HiP) basins during the July storm event. Hysteresis patterns are shown by connecting points throughout the storm, and arrows show the direction of the time-series

occur in these more waterlogged soils, but the saturated conditions and standing water prevent rapid infiltration.

In all watersheds, the rise in the groundwater component and decline in the organic component from July to September was consistent with active layer dynamics. As the active layer depth reached the mineral soils, water infiltration increased and greater flow was generated from deeper horizons. From July to September, the contribution of precipitation to streamflow increased in the burn and high-permafrost watersheds, but declined slightly in the low-permafrost watershed. We expected an increase in the precipitation component for all streams in response to higher precipitation intensity in September. Deeper infiltration of water into mineral soils with

greater  $\text{Ca}^{2+}$  concentration may underestimate the contribution of precipitation. Nevertheless, the trajectories for the DOC and  $\text{Ca}^{2+}$  relationship indicated that the organic component was more important in July (clockwise), whereas precipitation was more important during September (counter-clockwise).

#### Permafrost and chemistry

Consistent chemical responses among watersheds during storms demonstrate the importance of water flow paths and weathering processes in regulating stream chemistry.

Major cations ( $\text{Ca}^{2+}$ ,  $\text{Mg}^{2+}$ ,  $\text{K}^+$  and  $\text{Na}^+$ ) always declined with increasing discharge due to dilution of

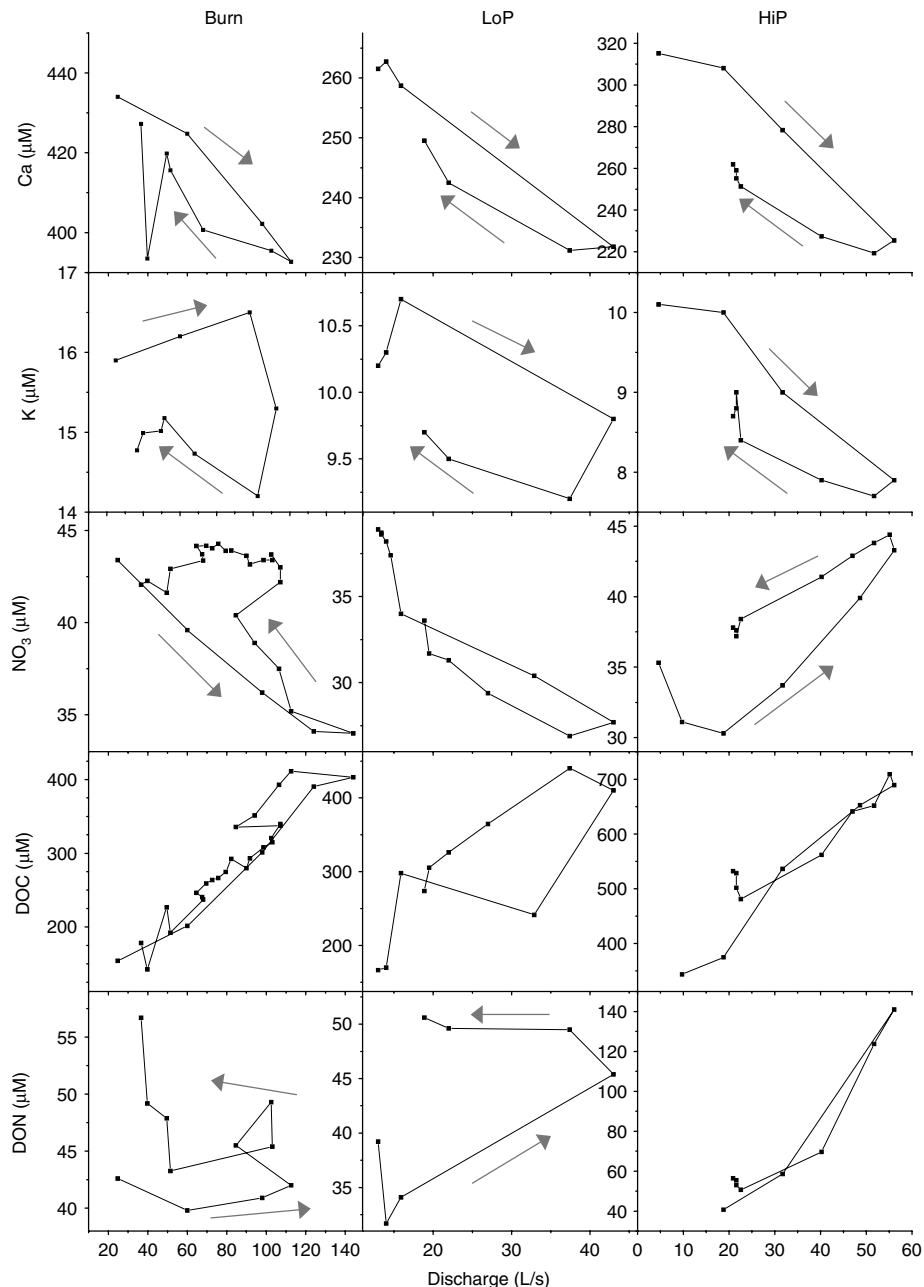


Figure 7. Concentration versus discharge plots of selected chemistry for the burn, low-permafrost (LoP) and high-permafrost (HiP) basins during the September storm event. Hysteresis patterns are shown by connecting points throughout the storm, and arrows show the direction of the time-series

baseflow water, which is enriched in weathering products, by precipitation and water from surface soils. The same surface flow paths that dilute major cations also enrich organic compounds. DOC and DON increased with storm discharge, suggesting that the mobilization of organic compounds in the active layer increases with streamflow.

Nitrate differences among watersheds can be attributed to biotic processes and flow paths governed by permafrost. Nitrate consistently decreased during storms in the low-permafrost watershed, but, simultaneously, increased with flow in the high-permafrost watershed. As our mixing model demonstrated, the storm water in the low-permafrost watershed was generated from a small contributing area confined to saturated valley-bottom soils. This water was a mixture of low nitrate precipitation

and anoxic soil water that dilutes stream nitrate concentrations during peak flows (Hill, 1993). In this way, the riparian zone in CPRW may be acting as a sink for dissolved nitrogen via processes such as denitrification and plant uptake (Peterjohn and Correll, 1994). An increase in nitrate with flow in the high-permafrost watershed suggests that permafrost-dominated hillslopes are potential sources of nitrate in sub-arctic regions. The contributing area for the high-permafrost watershed is much larger than in the low-permafrost watershed, including hillslopes and near stream valley-bottom zones. Hillslope water moves toward the stream after soils become saturated and generate lateral flow, leaching nitrate and organic compounds.

### Ecosystem implications

Since the nitrogen deposition rate is low in interior Alaska, biotic processes such as mineralization or nitrogen fixation must be supplying the nitrate flux to streams in the high-permafrost watershed during storms. Nitrogen fixation from symbiotic cyanobacterial (*Nostoc* sp.) is associated with feather moss (*Pleurozium schreberi*) in boreal forests of Scandinavia (1.5 to 2.0 kg ha<sup>-1</sup> year<sup>-1</sup> of nitrogen; DeLuca *et al.*, 2002). Feather moss is ubiquitous in permafrost-underlain hillslopes at CPRW and could potentially provide up to five times the rate of atmospheric deposition of nitrogen in CPRW. Nitrogen fixation by alder (*Alnus crispa* and *Alnus tenuifolia*) could also be a potential nitrate source, but alder is more common in deciduous stands than spruce stands at CPRW (Troth *et al.*, 1976). At CPRW, the bulk of stream nitrogen output is comprised of nitrate, and concentrations are an order of magnitude higher than published concentrations in other boreal (Ford and Naiman, 1989; Stottlemyer, 1992; Cooke and Prepas, 1998) and in arctic ecosystems (Peterson *et al.*, 1992). Given these high concentrations of nitrate in CPRW streams, it would require a widespread and severe fire disturbance in order to see a significant and long-term change in nitrate chemistry.

### CONCLUSIONS

Whereas antecedent moisture conditions largely control the soil contribution to flow in temperate, permafrost-free watersheds (DeWalle *et al.*, 1988; Hooper *et al.*, 1990), we found that the presence of permafrost and the active layer depth are also important factors governing the contribution of the soil system to stormflow. This results in a lag response of flow from the organic soils because they must become saturated before generating hillslope runoff. Consequently, organic soils can serve as a source for not only DOC and DON, but also DIN, mainly nitrate. If, in the future, active layer depths become deeper each season due to increasing ambient temperatures and a more frequent and severe fire regime, then organic soils could become an even more important source of nitrogen to sub-arctic streams. Additionally, movement of water from organic to mineral soils will result in a dissolution of weathering ions, such as calcium, and adsorption of DOC (MacLean *et al.*, 1999). The contributing area for stormflow and the chemistry of these source areas largely affects the chemistry of streams at CPRW. Storm chemistry in low-permafrost watersheds is influenced mainly by the saturated riparian soils and precipitation, whereas watersheds with greater permafrost coverage are affected by flow from more distant hillslopes underlain by permafrost that reaches the stream following saturation. In interior Alaska, less severe fires that do not affect riparian zones may only have a short-term effect on the water chemistry of receiving streams.

### ACKNOWLEDGEMENTS

We thank Joni Wilm, Jeremiah Drage, Ben Johnson, and Bob Bolton for assistance in the field, and Huan Luong for laboratory assistance. Three anonymous reviewers provided comments that greatly improved the manuscript. Support for this research was provided by the US National Science Foundation, Division of Environmental Biology, TECO program (DEB-9707461) and the National Science Foundation LTER program (DEB-9211769).

### REFERENCES

- Bayley SE, Schindler DW. 1991. The role of fire in determining water chemistry in northern coniferous forests. In *Ecosystem Experiments. SCOPE 45*, Mooney HA, Medina E, Schindler DW, Schulze ED, Walker BH (eds). Wiley: New York; 145–165.
- Bayley SE, Schindler DW, Beaty KG, Parker BR, Stinton MP. 1992. Effects of multiple fires on nutrient yields from stream draining boreal forest and fen watersheds: nitrogen and phosphorus. *Canadian Journal of Fisheries and Aquatic Sciences* **49**: 584–596.
- Beaty KG. 1994. Sediment transport in a small stream following two successive forest fires. *Canadian Journal of Fisheries and Aquatic Sciences* **51**: 2723–2733.
- Burn CR. 1998. The response (1958–1997) of permafrost and near-surface ground temperatures to forest fire, Takhini River valley, southern Yukon Territory. *Canadian Journal of Earth Sciences* **35**: 184–199.
- Chorover J, Vitousek PM, Everson DA, Esperanza AM, Turner D. 1994. Solution chemistry profiles of mixed-conifer forests before and after fire. *Biogeochemistry* **26**: 115–144.
- Cooke SE, Prepas EE. 1998. Stream phosphorus and nitrogen exports from agricultural and forested watersheds on the Boreal Plain. *Canadian Journal of Fisheries and Aquatic Sciences* **55**: 2292–2299.
- DeLuca TH, Zackrisson O, Nilsson M-C, Sellstedt A. 2002. Quantifying nitrogen-fixation in feather moss carpets of boreal forests. *Nature* **419**: 917–920.
- DeWalle DR, Swistock BR, Sharpe WE. 1988. Three-component tracer model for stormflow on a small Appalachian forested catchment. *Journal of Hydrology* **104**: 301–310.
- Eshleman KN, Pollard JS, O'Brien AK. 1993. Determination of contributing areas for saturation overland flow from chemical hydrograph separations. *Water Resources Research* **29**: 3577–3587.
- Evans C, Davies TD. 1998. Causes of concentration/discharge hysteresis and its potential as a tool for analysis of episodic hydrochemistry. *Water Resources Research* **34**: 129–137.
- Flannigan MDF, Van Wagner CE. 1991. Climate change and wildfire in Canada. *Canadian Journal of Forest Research* **21**: 66–72.
- Ford TE, Naiman RJ. 1989. Groundwater–surface water relationships in boreal forest watersheds: dissolved organic carbon and inorganic nutrient dynamics. *Canadian Journal of Fisheries and Aquatic Sciences* **46**: 41–49.
- Gordon JD. 1999. *External quality-assurance results for the National Atmospheric Deposition Program/National Trends Network, 1995/1996*. USGS Water Resources Investigations Report 99–4072, Denver, CO.
- Haugen RK, Slaughter CW, Howe KE, Dingman SL. 1982. *Hydrology and climatology of the Caribou-Poker Creeks Research Watershed, Alaska*. CRREL Report 82-26.
- Hill AR. 1993. Nitrogen dynamics of storm runoff in the riparian zone of a forested watershed. *Biogeochemistry* **20**: 19–44.
- Hinzman LD, Fukuda M, Sandberg DV, Chapin III FS, Dash D. 2003. FROSTFIRE: an experimental approach to predicting the climate feedbacks from the changing boreal fire regime. *Journal of Geophysical Research* **108**: 8153.
- Hinzman LD, Bolton WR, Petrone KC, Jones JB Jr, Adams PC. 2006. Watershed hydrology and chemistry in the Alaskan boreal forest: the central role of permafrost. In *Alaska's Changing Boreal Forest*, Chapin FS III, Oswood MW, Van Cleve K, Viereck LA, Verbyla DL (eds). Oxford University Press: New York; 269–284.
- Hooper RP, Shoemaker CA. 1986. A comparison of chemical and isotopic hydrograph separation. *Water Resources Research* **22**: 1444–1454.

- Hooper RP, Christophersen N, Peters NE. 1990. Modeling streamwater chemistry as a mixture of soilwater end-members—an application to the Panola Mountain catchment, Georgia, U.S.A. *Journal of Hydrology* **116**: 321–343.
- McNamara JP, Kane DL, Hinzman LD. 1997. Hydrograph separations in an Arctic watershed using mixing model and graphical techniques. *Water Resources Research* **33**: 1707–1719.
- MacLean R, Oswood MW, Irons III JG, McDowell WH. 1999. The effect of permafrost on stream biogeochemistry: a case study of two streams in the Alaskan (USA) taiga. *Biogeochemistry* **47**: 239–267.
- Mulholland PJ. 1993. Hydrometric and stream chemistry evidence of three storm flowpaths in Walker Branch Watershed. *Journal of Hydrology* **151**: 291–316.
- Murphy J, Riley JP. 1962. A modified single solution method for the determination of phosphate in natural waters. *Analytica Chimica Acta* **27**: 31–36.
- Osterkamp TE, Romanovsky VE. 1999. Evidence for warming and thawing of discontinuous permafrost in Alaska. *Permafrost and Periglacial Processes* **10**: 17–37.
- Peterjohn WT, Correll DL. 1994. Nutrient dynamics in an agricultural watershed: observations on the role of a riparian forest. *Ecology* **65**: 1466–1475.
- Peterson BJ, Corliss T, Kriet K, Hobbie JE. 1992. Nitrogen and phosphorus concentrations and for the upper Kuparak River on the North Slope of Alaska in 1980. *Hydrobiologia* **240**: 61–69.
- Ray Sr. 1988. *Physical and chemical characteristics of headwater streams at Caribou–Poker Creeks Research Watershed*. MS thesis, University of Alaska Fairbanks, Fairbanks, AK.
- Richter DD, Ralston CW, Harms WR. 1982. Prescribed fire: effects on water quality and forest nutrient cycling. *Science* **215**: 661–663.
- Rieger S, Furbush CE, Schoephorster DB, Summerfield H, Geiger Jr LC. 1972. *Soils of the Caribou–Poker Creeks Research Watershed, interior Alaska*. CRREL Technical Report 236, US Army Corps of Engineers, Cold Regions Research and Engineering Laboratory, Hanover, NH.
- Schindler DW, Newbury RW, Beaty KG, Prokopowich J, Rusczyński T, Dalton JA. 1980. Effects of windstorm and forest fire on chemical losses from forested watersheds and on the quality of receiving streams. *Canadian Journal of Fisheries and Aquatic Sciences* **37**: 328–334.
- Sklash MG, Farvolden RN. 1979. The role of groundwater in event runoff. *Journal of Hydrology* **43**: 45–65.
- Sklash MG, Farvolden RN, Fritz P. 1976. A conceptual model of watershed response to rainfall, developed through the use of oxygen-18 as a natural tracer. *Canadian Journal of Earth Sciences* **13**: 271–283.
- Sokal RR, Rohlf FJ. 1994. *Biometry: The Principles and Practice of Statistics in Biological Research*. W.H. Freeman: San Francisco.
- Solorzano L. 1969. Determination of ammonia in natural waters by the phenylhypochlorite method. *Limnology and Oceanography* **14**: 799–801.
- StatSoft. 2000. *STATISTICA for Windows*. StatSoft, Inc., Tulsa, OK.
- Stottlemeyer R. 1992. Nitrogen mineralization and streamwater chemistry, Rock Creek watershed, Denali National Park, Alaska, U.S.A. *Arctic and Alpine Research* **24**: 291–303.
- Troth JL, Deneke FJ, Brown LM. 1976. Upland aspen/birch and black spruce stands and their litter and soil properties in interior Alaska. *Forest Science* **22**: 33–44.
- White D, Yoshikawa K, Garland DS. 2002. Use of dissolved organic matter to support hydrologic investigations in a permafrost-dominated watershed. *Cold Regions Science and Technology* **35**: 27–33.
- Williams MR, Brown AD, Melack JM. 1997. Geochemical and hydrologic controls on the composition of surface water in a high-elevation basin, Sierra Nevada, California. *Limnology and Oceanography* **38**: 775–797.
- Williams MR, Melack JM. 1997. Effects of prescribed burning and drought on the solute chemistry of mixed-conifer forest streams of the Sierra Nevada, California. *Biogeochemistry* **39**: 225–253.
- Woo MK. 1986. Permafrost hydrology in North America. *Atmosphere–Ocean* **24**: 201–234.
- Wood ED, Armstrong FAJ, Richards FA. 1967. Determination of nitrate in seawater by cadmium-copper reduction to nitrite. *Journal of the Marine Biological Association of the United Kingdom* **47**: 23–31.
- Wright RF. 1976. The impact of forest fire on the nutrient influxes to small lakes in northeastern Minnesota. *Ecology* **57**: 649–663.
- Yoshikawa K, Hinzman LD, Gogineni P. 2002. Ground temperature and permafrost mapping using an equivalent latitude/elevation model. *Journal of Glaciology and Geocryology* **24**: 526–531.